Wideband Microstrip Leaky-Wave Antennas With Two Symmetrical Side Beams for Simultaneous Dual-Beam Scanning

Debabrata K. Karmokar, *Member, IEEE*, Karu P. Esselle, *Fellow, IEEE*, and Trevor S. Bird, *Life Fellow, IEEE*

***Abstract*—Wideband microstrip leaky-wave antennas (LWAs) that radiate two symmetrical side beams are described. The two beams are steered simultaneously by sweeping the operating frequency. To achieve this, the second higher order mode of the microstrip is excited. Two electric field nulls are created between the microstrip and the ground plane using via arrays to suppress lower order modes. To test the concept, one of the antenna designs was prototyped. The prototyped antenna is capable of steering two symmetrical beams within a range of 37° when frequency is swept between 6.92 and 8.75 GHz. The measured peak gain of the antenna is 12.7 dBi and the variation of gain from 6.92 to 8.75 GHz is 3.1 dB. The measured 10-dB return loss bandwidth is 23%, which is very large for a dual-beam microstrip LWA. Such a wide impedance bandwidth is essential to achieve beam scanning over a wide angular range by sweeping frequency. Another advantage is that this single-layer antenna is easy to fabricate.**

***Index Terms*—Dual beam, microstrip, leaky-wave antennas (LWAs), higher order mode, second higher order, beam scanning.**

I. Introduction

A MICROSTRIP leaky-wave antenna (LWA) was demonstrated in the late 1970s [1] using the first higher order mode of a microstrip line, with methods to excite that mode. Since then the radiation properties of microstrip higher order modes have attracted research interest [2], [3], microstrip LWAs are attractive due to their advantages such as planar low profile, ease of fabrication, high gain, large bandwidth, and inherent beam-scanning capabilities [4]–[9]. A LWA can reduce system complexity in applications such as multipoint communications and surveillance [10]. A variety of research has been conducted on LWAs. Recent LWAs that produce a single beam include a metamaterial-based dominant-mode LWA [11], a multilayered composite right/left-handed (CRLH) LWA [12], a periodic half-width microstrip LWA [13], a double-periodic CRLH substrate-integrated waveguide (SIW) LWA [14], a SIW LWA with H-shaped slots [15], a microstrip LWA loaded with shorted stubs [16], a half-width microstrip LWA with periodic short circuits [17], a periodic phase-reversal LWA [18], a coupled half-width microstrip leaky EH_1-mode antenna [19], a half-width microstrip LWA with edge loading [20], a half-mode SIW LWA [21], a half-mode SIW circularly polarized LWA [22], a substrate-integrated CRLH LWA with two leaky-wave radiator elements [23], a butterfly SIW LWA [24], a SIW LWA for endfire radiation [25], a SIW LWA with transverse slots [26], a 1-D Fabry-Perot LWA [27], and a conformal tapered LWA [28]. A number of LWAs that can produce two simultaneously scanning beams, one in the forward direction and the other in the backward direction, have been reported [29]–[31].

Nevertheless, only limited research has been reported on achieving two side beams. Two feed structures were proposed to excite the second higher order mode of a microstrip line to make such a LWA [32]. One of them is a coplanar waveguide (CPW) on the same plane as the microstrip, and the other is also a CPW but on the ground plane. Both designs have two slots at each end of the microstrip. A microstrip-fed second higher order mode LWA was proposed for dual-beam application in [10]. In this approach, each end of the microstrip was provided with two tuned quarter-wavelength slots and two vias, which are located a quarter width away from each microstrip edge to create two electric field nulls. An aperture-coupled second higher order mode microstrip LWA has been proposed to produce dual beams [33]. In order to launch this mode, the ground plane was modified by etching two narrow slots leaving half a guided wavelength spacing between them (the guided wavelength is the wavelength of the coupled microstrip). A microstrip LWA has been designed for second higher order mode operation in [34] using the same method of excitation as in [33]. A micro-CPW LWA has been proposed in [35] with two symmetrical side beams for dual-beam operation. This antenna consists of a microstrip line on one surface of the substrate and a CPW on the other surface. Most of the LWAs that produce dual beams with second higher order mode excitation have bandwidth limitations.

This paper presents an approach to achieve wideband microstrip LWAs with two tilted symmetrical side beams. Both edges of the microstrip line are used as radiating elements, and the beams are steered simultaneously by sweeping frequency. This second higher order antenna makes use of a simple technique to produce two symmetrical side beams without any special feed mechanisms.

Manuscript received May 08, 2015; revised December 01, 2015; accepted January 12, 2016. Date of publication February 12, 2016; date of current version April 05, 2016. This work was supported in part by the Australian Research Council (ARC) and in part by the International Postgraduate Research Scholarship (IPRS).

The authors are with the Centre for Collaboration in Electromagnetic and Antenna Engineering, Department of Engineering, Faculty of Science and Engineering, Macquarie University, Sydney, NSW-2109, Australia (e-mail: dkkarmokar@ieee.org; karu@ieee.org; ts.bird@ieee.org).

Color versions of one or more of the figures in this paper are available online at http://ieeexplore.ieee.org.

Digital Object Identifier 10.1109/TAP.2016.2529646

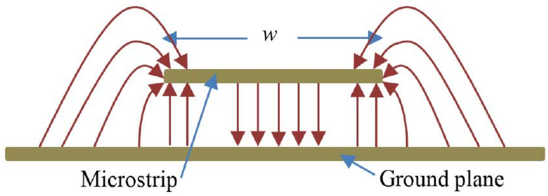

Fig. 1. Electric-field distributions of the second higher order mode (EH_2) of a microstrip line (substrate omitted).

The fundamental mode (EH_0) of a uniform microstrip line does not radiate at lower frequencies because the electric field is strongly bound to the microstrip line and the ground plane. Some higher order modes of microstrip lines radiate as leaky waves. The first higher order mode has a phase reversal and an electric field null at the center. Fig. 1 shows the field distributions of the second higher order (EH_2) mode of a microstrip line which has two phase reversals and two nulls that are approximately *w/4* away from the edges, where *w* is the width of the microstrip. The half-width microstrip LWA proposed in [36] operates in the first higher order mode of the microstrip line. It presents a very simple yet effective technique to excite a microstrip line in the first higher order mode that is to introduce a septum (conducting wall) along the center of the microstrip to create an electric field null at the center. This suppresses the fundamental mode and excites the first higher order mode. Likewise, two arrays of vias are employed here to suppress EH_0 and EH_1 modes and to excite the EH_2 mode.

II. Antenna Configuration

The generic configuration that is common to all LWAs presented in this paper is illustrated in Fig. 2(a)–(c), and their 3-D radiation pattern for a particular frequency is shown in Fig. 2(d). A "very long" LWA with a microstrip length (l) of $12\lambda_0$ is considered as the reference antenna for comparison purposes, where λ_0 is the free-space wavelength at 8 GHz. The prototyped and tested LWA has a reduced strip length (l) of about $6\lambda_0$. All antennas were designed and optimized using CST Microwave Studio. The prototyped antenna was printed on a Rogers RT5880 substrate with a thickness of 1.575 mm, a dielectric constant of 2.2, and a loss tangent of 0.0009. The length (L) and width (W) of the substrate are 254 mm ($6.77\lambda_0$) and 90 mm ($2.4\lambda_0$), respectively.

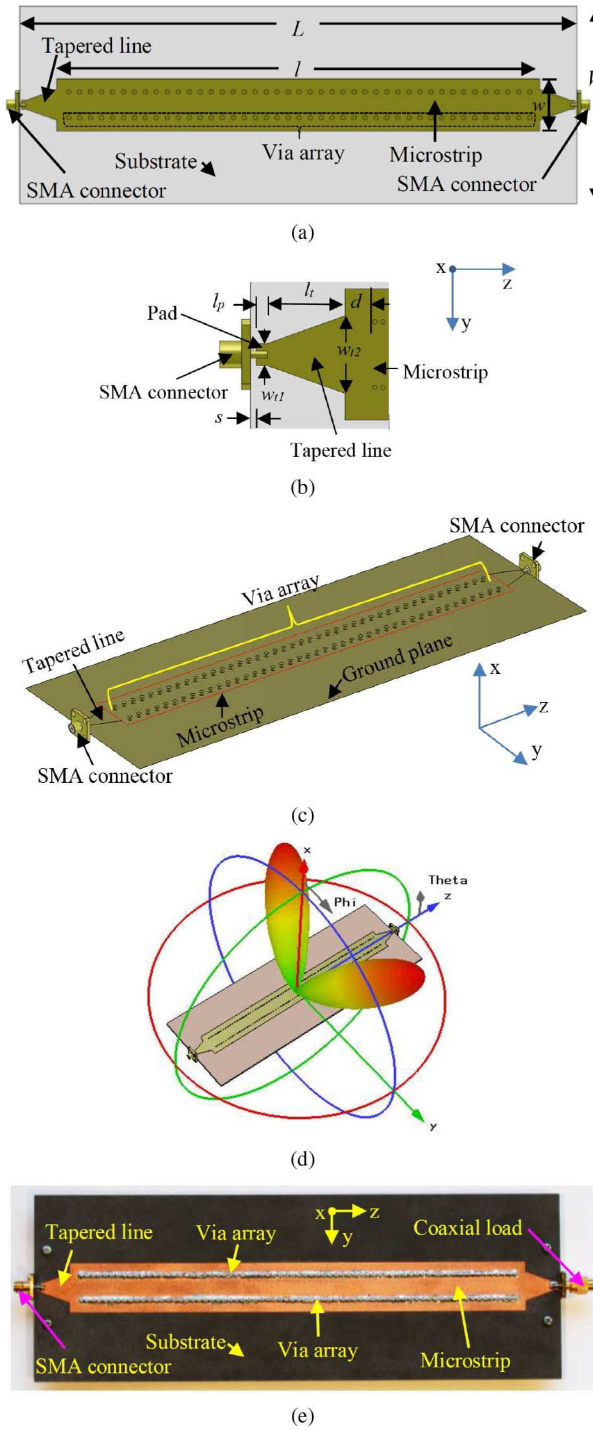

Fig. 2. Dual-beam microstrip LWA. (a) Top view (not to scale). (b) Feed section. (c) Perspective view (substrate and microstrip omitted, not to scale). (d) 3-D radiation pattern of the antenna. (e) Top view of the fabricated prototype.

A. Radiating Element

The length (l) and width (w) of the microstrip line are 220 mm ($5.87\lambda_0$) and 24 mm ($0.64\lambda_0$), respectively. It was designed to produce two side beams with a simple feed technique. Two arrays of vias (Fig. 2) are placed *w/4* away from each edge, to create two electric field nulls between the microstrip and ground plane.

B. Feed Section

The antenna is fed by the tapered line shown in Fig. 2(b). To achieve good impedance matching and a wide impedance bandwidth, the dimensions of the tapered line have been optimized through some parametric studies. The optimum length (l_t), width (w_{t1}) at the feed end, and width (w_{t2}) at the microstrip end of the tapered line are 14, 4, and 14 mm, respectively.

In order to connect the SMA pin to the tapered line, a small pad was provided at each end [Fig. 2(b)]. The width of each

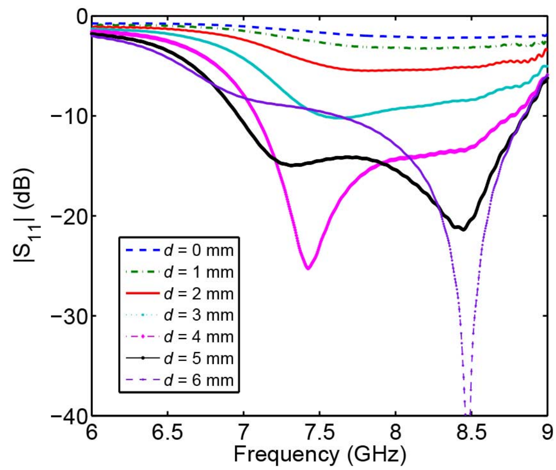

Fig. 3. Variation of reflection coefficient with the gap (d). $w_{t1} = 4$ mm; $w_{t2} = 14$ mm; $l_t = 14$ mm.

pad is the same as the width (w_{t1}) of the tapered line at the feed end, and the length (l_p) of each pad is 2 mm. There is a narrow spacing ($s = 1$ mm) between the SMA connector and the pad. This spacing was introduced to avoid an unwanted short circuit between the SMA pin and the SMA ground by the pad, as the pad width (4 mm) is very close to the diameter of the Teflon section in the SMA connector, which is 4.1 mm.

C. Via Arrays

An appropriate gap (d) is required between the feed and the first via, as shown in Fig. 2(b), to force the wave toward the microstrip edges, as well as to improve impedance matching. Initial designs of this antenna had two septa, each 0.8 mm wide, placed *w/4* away from each edge. When compared with via arrays, septa demand less computer resources for full-wave simulations and parameter analyses. Fig. 3 shows the variation of $|S_{11}|$ with d. It can be seen that the best bandwidth is obtained when d is 5 mm. In the final design, the two septa were replaced by two arrays of vias as shown in Fig. 2, for ease of fabrication using in-house facilities. There are a total of 141 vias to emulate each septum. The diameter of each via is 0.8 mm and the center-to-center distance between two adjacent vias is 1.5 mm. The center of the first via of each array is 5.4 mm away from the feed end of the microstrip.

D. Final Prototype

The prototype that was fabricated is shown in Fig. 2(e). The microstrip is fed from one end through the tapered line, and a 50-Ω coaxial load is connected to the other end of the microstrip to suppress any reflected wave. In the simulations, the SMA connectors were modeled according to the actual dimensions of a commercially available SMA connector. Modeling of SMA connectors in the full-wave simulation reduces the discrepancy between predicted and measured results. Waveguide ports were used to excite the SMA connectors in CST. The diameter of the inner conductor of each SMA connector is 1.28 mm, and the inner diameter of the outer conductor is 4.1 mm.

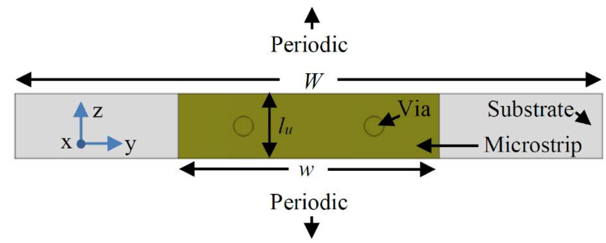

Fig. 4. Unit cell (not to scale) used to obtain the dispersion diagram of an infinitely long antenna.

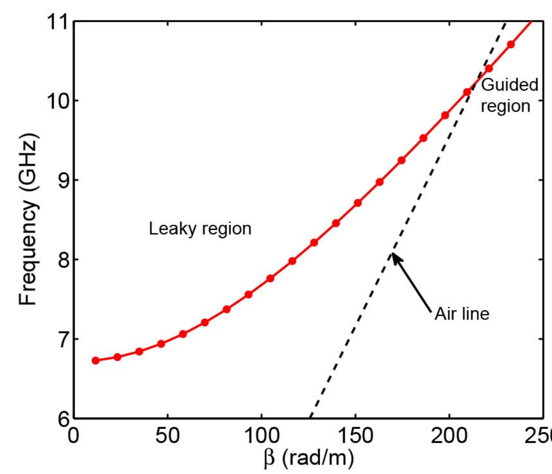

Fig. 5. Dispersion diagram of an infinitely long LWA.

III. Unit Cell and Dispersion Diagram

To understand the leaky mode operation, consider initially the dispersion diagram of the relevant mode. The unit cell used to obtain the dispersion characteristics, by solving an eigenmode problem, is shown in Fig. 4. This unit cell is repeated in the z-direction. The width (W) of the ground plane and substrate and the width (w) of the microstrip line are the same as in the final design, whereas the length (l_u) of the unit cell, i.e., the center-to-center distance between two adjacent vias, is 1.5 mm. Fig. 5 shows the dispersion diagram of the unit cell obtained using the CST EM Eigenmode solver. At $\pm$z-direction periodic boundaries, a variable phase shift has been applied. By running a parameter sweep on the phase shift and plotting the calculated eigenmodes as a function of the phase shift, the propagation constant has been extracted. In Fig. 5, the dotted line is the air line, given by $k_0 = \omega\sqrt{\varepsilon_0\mu_0}$. The guided wave becomes leaky when $\beta/k_0 < 1$, where β is the phase constant.

For an infinitely long LWA, the direction of the main beams can be predicted from the dispersion diagram. It is a function of frequency given by [37]

$$\theta(f) = \cos^{-1}\left[\frac{\beta(f)}{k_0(f)}\right] \tag{1}$$

where $k_0(f)$ is the free-space wave number and $\theta(f)$ is the angle measured from the antenna axis (z-axis). Fig. 6 represents the beam direction as a function of frequency, predicted from two different methods: 1) from the dispersion diagram and 2) from full-wave simulation of three antennas with different microstrip lengths. Full-wave simulations were conducted

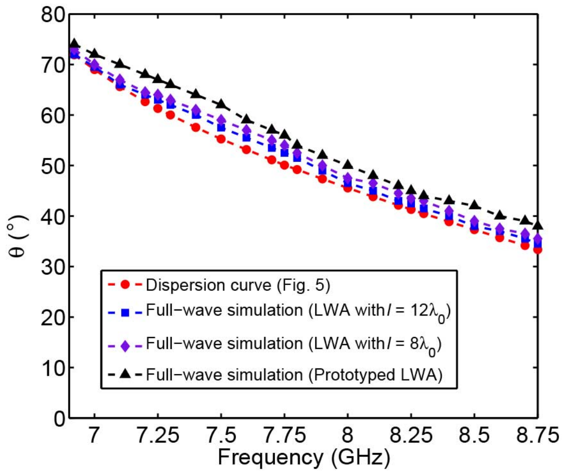

Fig. 6. Main beams direction, predicted from the dispersion diagram and full-wave simulations.

using the time-domain solver in CST. Apart from the length, all the dimensions of the three antennas are the same (identical to the antenna prototype). It can be seen from Fig. 6 that the predicted beam directions from the dispersion curve and from the full-wave simulations are in agreement. There is a small difference between the curves because the dispersion diagram solution applies for an infinite number of unit cells. The difference is larger for the short antenna. This discrepancy between the dispersion diagram and full wave simulation can be attributed to the existence of a small backward leaky wave due to the finite length. Increasing the number of unit cells in the antenna, i.e., increasing the antenna length, weakens the backward wave and hence reduces the deviation between the predictions. The two antennas with long microstrip lines were simulated to verify this. When the length of the microstrip (l) is increased to $8\lambda_0$, keeping all other dimensions the same, the difference between full-wave and dispersion-based prediction decreases. With further extension of the length to $12\lambda_0$, the difference reduces significantly as shown in Fig. 6. The present study shows that the beam direction (θ) of a dual-side-beam scanning LWA can be predicted from the dispersion diagram.

IV. Measured and Predicted Results

A. S-Parameters

The antenna is fed from one end by the SMA connector through the tapered line. The S-parameters of the dual-beam antenna were measured using an Agilent PNA-X N5242A network analyzer. Fig. 7 shows the measured S-parameters together with the predicted results. It can be seen that the measured and predicted values are in good agreement. The slight variation occurs due to fabrication tolerances. The measured return loss is greater than 10 dB from 6.92 to 8.72 GHz. Then it drops below 10 dB, but remains ≥ 9 dB till 8.75 GHz. The measured and predicted curves of the forward transmission coefficient (S_{21}) are also shown in Fig. 7. Once again, they agree very well in the matched bandwidth of the antenna.

At the lower limit of the return loss bandwidth, isolation is very high, which means that most of the power radiates. Close to the upper end around 8.75 GHz, isolation is less yet only a small amount of the incident power is absorbed by the load, i.e., a sufficiently large amount of power radiates.

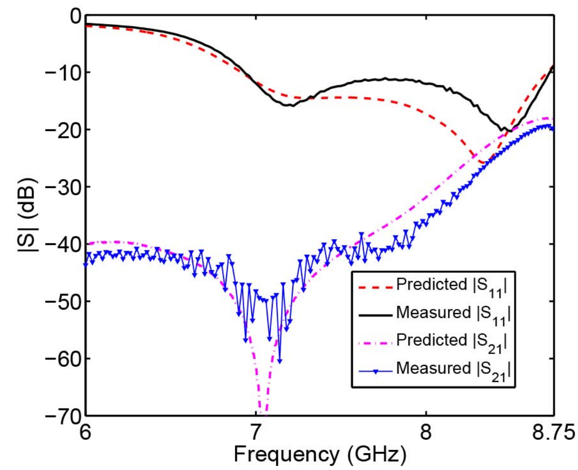

Fig. 7. Predicted and measured S-parameters of the dual-beam LWA.

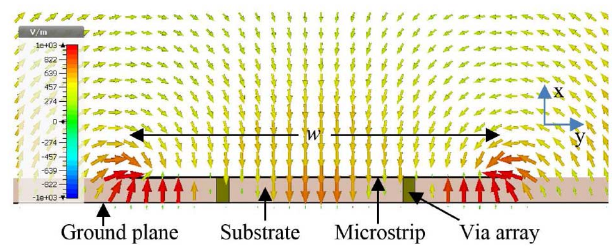

Fig. 8. Electric field orientation in the xy-plane (10 mm away from the feed end of the microstrip toward +z-axis) at 7 GHz.

B. Electric Field Distribution

Electric field distribution across the antenna was investigated to verify the mode of operation. Fig. 8 shows the transverse electric field vectors of the antenna on a cross section that is 10 mm away from the feed end of the microstrip. Note that two electric field nulls are created by via arrays, which are placed *w/4* away from the edges. The electric field inside the substrate has a phase reversal at each via array, mimicking the ideal second higher order mode of a microstrip line, as shown in Fig. 1.

C. Leakage Rate

The measured and predicted leakage rates of the prototype antenna that have been obtained using the method in [38], are shown in Fig. 9. It shows that the leakage rate is high at lower frequencies, where most of the power radiates from a short section at the feed end of the microstrip. This makes the effective radiating aperture short and results in larger beamwidth, lower directivity, and lower gain. With an increase of frequency, leakage rate decreases and input power propagates toward the load end, producing a long effective aperture, decreasing the beamwidth and increasing the directivity. When the microstrip is long enough, most of the power radiates before

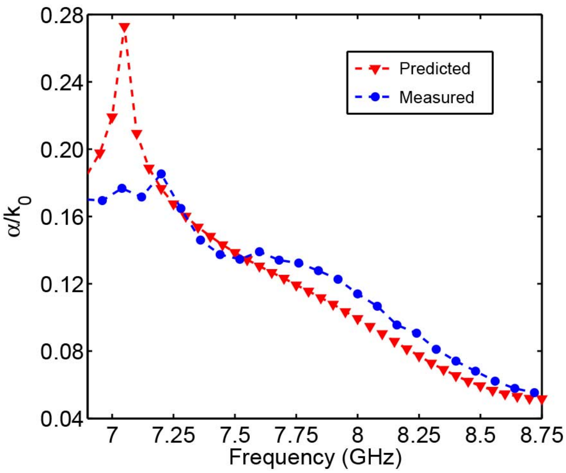

Fig. 9. Predicted and measured leakage constant (α/k_0) of the prototyped antenna as a function of frequency.

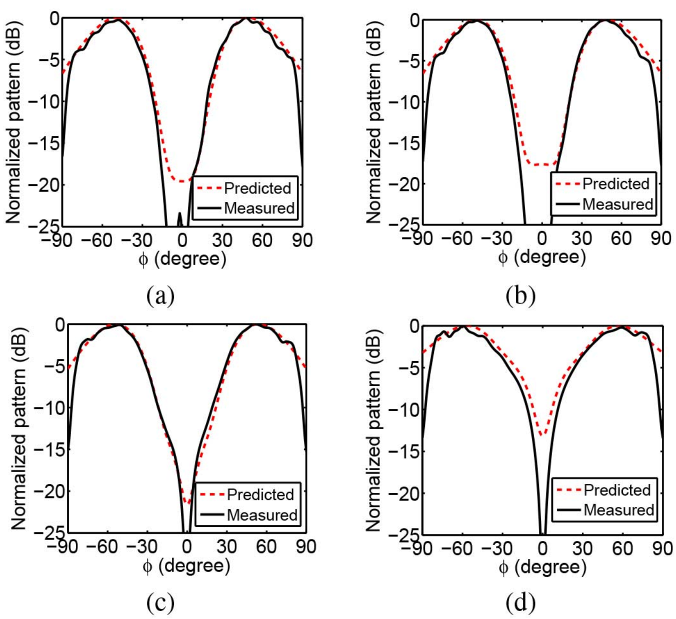

Fig. 10. Predicted and measured radiation patterns (normalized) on constant-θ cones at (a) f = 7 GHz (on $\theta = 73°$ cone), (b) f = 7.5 GHz (on $\theta = 66°$ cone), (c) f = 8.25 GHz (on $\theta = 48°$ cone), and (d) f = 8.75 GHz (on $\theta = 38°$ cone).

reaching the load; otherwise, some power will be dissipated in the load. Although the longer antennas preform better at high frequencies, they may be too long for some practical applications.

D. Radiation Pattern

The radiation characteristics were measured using the NSI700S-50 spherical near-field antenna range at the Australian Antenna Measurement Facility (AusAMF) at CSIRO, Marsfield. The antenna was placed vertically for the measurements to align it with the probe since it is polarized in the y-direction [Fig. 2(e)]. The measured normalized E-plane radiation patterns for four different frequencies are shown in Fig. 10 together with the predicted values. These patterns are on constant-θ cones, and the cone angle θ has

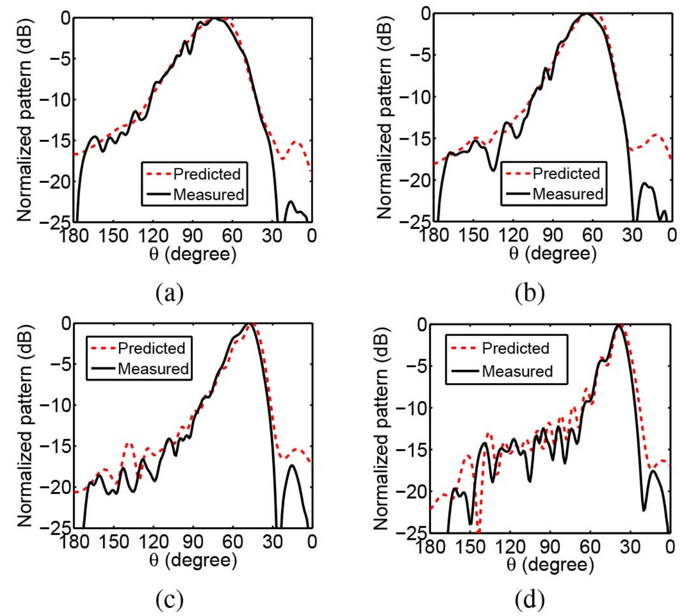

Fig. 11. Predicted and measured radiation patterns (normalized) on constant-ϕ planes at (a) f = 7 GHz (on $\phi = 48°$ plane), (b) f = 7.5 GHz (on $\phi = 48°$ plane), (c) f = 8.25 GHz (on $\phi = 51°$ plane), and (d) f = 8.75 GHz (on $\phi = 60°$ plane). Similar patterns are exist for negative ϕ planes. Note that angle "θ" is measured from the z-axis as shown in Fig. 2.

been chosen to pass through the peak of each 3-D beam. The predicted and measured patterns are in good agreement for all frequencies shown. It can be seen that the antenna produces two symmetrical beams to the sides, in (θ; $\pm\phi$) directions. Moreover, the beamwidths on constant-θ cones are almost the same [Fig. 10 (a)–(d)] throughout the frequency range from 6.92 to 8.75 GHz. At 7 GHz, one of the measured main beams points at $\phi = 48°$ while the other points at $\phi = -48°$. It was observed that at low frequencies, the beam directions ($\pm\phi$) on constant-θ cones do not change with frequency; however, it changes slightly at higher frequencies. The change of the main beam direction on constant-θ cones is small (13° within the bandwidth), considering the wide beamwidth.

Fig. 11 shows the normalized measured and predicted radiation patterns on constant-ϕ planes, at the same four frequencies as in Fig. 10. The radiation pattern cuts are shown for positive-ϕ planes; similar patterns exist on corresponding negative-ϕ planes also. Again the ϕ values for each cut have chosen such that the cut passes through the beam peak. The measured and predicted radiation patterns on constant-ϕ plane agree extremely well. At lower frequencies, the main beams point away from the antenna axis [Fig. 11(a)]. As the frequency increases, they move toward the antenna axis, which is an inherent property of LWAs. The beam direction (θ) of a LWA is given by (1). The value of β/k_0 changes with frequency and hence the beam direction. As expected from the analysis in Section IV-C, the beamwidth at 7 GHz (Fig. 11) is large on the constant-ϕ plane. However, with the increase of frequency, it becomes narrower. The beams at higher frequencies are very narrow as shown in Fig. 11(d).

In order to describe the 3-D shape of the radiation pattern, the measured normalized patterns at 6.92 and 8 GHz are shown

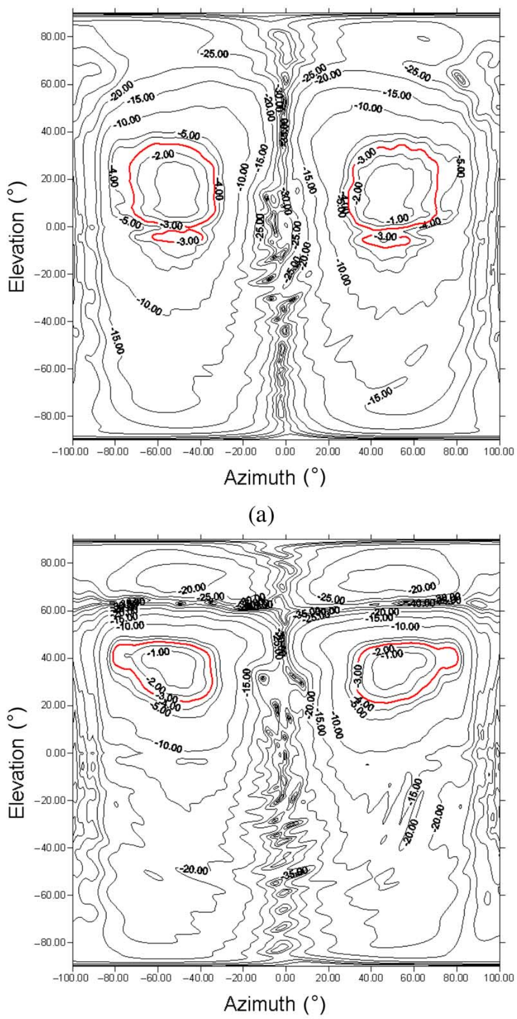

Fig. 12. Measured and normalized 2-D radiation patterns of the dual-beam antenna at (a) 6.92 GHz and (b) 8 GHz. The red contour corresponds to −3 dB.

TABLE I
MEASURED AND PREDICTED MAIN BEAM DIRECTIONS AT DIFFERENT FREQUENCIES

Frequency (GHz)	Main beam direction θ		ϕ	
	Measured	Predicted	Measured	Predicted
6.92	75°	74°	±48°	±50°
7.0	73°	72°	±48°	±50°
7.25	68°	67°	±48°	±50°
7.5	66°	62°	±48°	±51°
7.75	59°	56°	±47°	±52°
8.0	52°	50°	±51°	±54°
8.25	48°	45°	±51°	±55°
8.5	43°	42°	±61°	±56°
8.75	38°	38°	±60°	±57°

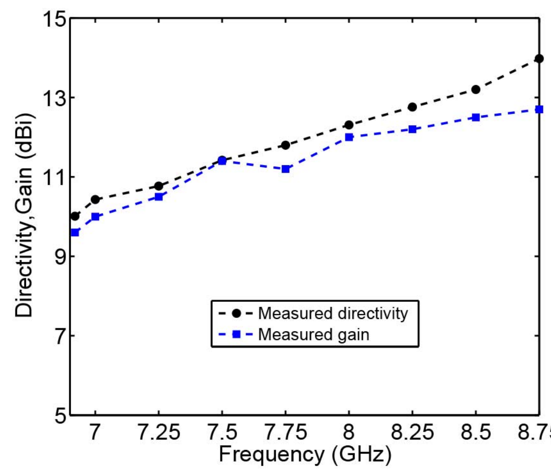

Fig. 13. Measured gain and directivity of the dual-beam LWA.

in Fig. 12 as a contour plot. It can be seen that the antenna produce two side beams with a null on the xz-plane. The measured and predicted beam directions for several frequencies are given in Table I. It can be seen that there is a very good agreement between them. The maximum deviation between the predicted and measured beam directions (θ) is less than 4°. This deviation at 7.5 GHz is negligible since the beamwidth is large (measured 3-dB beamwidth is 30°). Although the beams in higher frequencies are narrow, the predicted and measured beam directions match very well.

E. Measured Gain and Directivity

Fig. 13 shows the measured gain and directivity from 6.92 to 8.75 GHz. The directivity at 6.92 GHz is low compared to the directivity at higher frequencies, as expected. It can be seen from Fig. 11 that as the frequency increases, the beamwidth decreases, and hence, the directivity increases. The gain was measured using the gain comparison method. Similarly to the directivity, the gain increases with frequency. The maximum measured gain is 12.7 dBi and the variation of the gain is 3.1 dB between 6.92 and 8.75 GHz. Moreover, the gain is greater than 10 dBi from 7 to 8.75 GHz. Even though the return loss is 9 dB, the antenna still has the maximum gain at 8.75 GHz due to the large effective aperture and high directivity.

V. CONCLUSION

Wideband microstrip LWAs were designed to achieve two tilted symmetrical side beams for simultaneous dual-beam scanning. An understanding of the fundamental characteristics of the high-order microstrip modes has been used to excite radiating leaky modes. Two shorting walls were implemented using via arrays to produce two electric field nulls along the length of the microstrip line. The wide impedance bandwidth (23%) of the proposed LWAs allows for an increased range of frequency sweeping, which results in increased beam scanning range of symmetrical side-beam LWAs. The measured beam scanning range (θ; $\pm\phi$) of the prototyped antenna from 6.92 to 8.75 GHz is (75°; ±48°) to (38°; ±60°). The measured maximum gain of the antenna is 12.7 dBi, and the gain is greater than 10 dBi from 7 to 8.75 GHz.

References

[1] W. Menzel, “A new travelling wave antenna in microstrip,” in *Proc. 8th Eur. Microw. Conf.*, Sep. 1978, pp. 302–306.

[2] H. Ermert, “Guiding and radiation characteristics of planar waveguides,” *IEE Microw. Opt. Acoust.*, vol. OA-3, no. 2, pp. 59–62, Mar. 1979.

[3] A. A. Oliner, “Leakage from higher modes on microstrip line with application to antennas,” *Radio Sci.*, vol. 22, no. 6, pp. 907–912, 1987.

[4] D. R. Jackson, C. Caloz, and T. Itoh, “Leaky-wave antennas,” *Proc. IEEE*, vol. 100, no. 7, pp. 2194–2206, Jul. 2012.

[5] D. R. Jackson and A. A. Oliner, “Leaky-wave antennas,” in *Modern Antenna Handbook*, C. A. Balanis, Ed. Hoboken, NJ, USA: Wiley, 2008, ch. 7.

[6] D. K. Karmokar, K. P. Esselle, and T. S. Bird, “An array of half-width microstrip leaky-wave antennas radiating on boresight,” *IEEE Antennas Wireless Propag. Lett.*, vol. 14, pp. 112–114, Jan. 2015.

[7] Q. Lai, C. Fumeaux, and W. Hong, “Periodic leaky-wave antennas fed by a modified half-mode substrate integrated waveguide,” *IET Microw. Antennas Propag.*, vol. 6, no. 5, pp. 594–601, Apr. 2012.

[8] D. K. Karmokar, D. N. P. Thalakotuna, K. P. Esselle, and M. Heimlich, “Controlling the beam scanning limits of a microstrip leaky-wave antenna,” in *Proc. IEEE Antennas Propag. Soc. Int. Symp. (APSURSI)*, Jul. 2013, pp. 1330–1331.

[9] S. K. Podilchak, A. P. Freundorfer, and Y. M. M. Antar, “Broadside radiation from a planar 2-D leaky-wave antenna by practical surface-wave launching,” *IEEE Antennas Wireless Propag. Lett.*, vol. 7, pp. 517–520, Dec. 2008.

[10] T.-L. Chen, Y.-D. Lin, and J.-W. Sheen, “Microstrip-fed microstrip second higher order leaky-mode antenna,” *IEEE Trans. Antennas Propag.*, vol. 49, no. 6, pp. 855–857, Jun. 2001.

[11] L. Liu, C. Caloz, and T. Itoh, “Dominant mode leaky-wave antenna with backfire-to-endfire scanning capability,” *Electron. Lett.*, vol. 38, no. 23, pp. 1414–1416, Nov. 2002.

[12] Nasimuddin, Z. N. Chen, and X. Qing, “Multilayered composite right/left-handed leaky-wave antenna with consistent gain,” *IEEE Trans. Antennas Propag.*, vol. 60, no. 11, pp. 5056–5062, Nov. 2012.

[13] Y. Li, Q. Xue, E. K.-N. Yung, and Y. Long, “The periodic half-width microstrip leaky-wave antenna with a backward to forward scanning capability,” *IEEE Trans. Antennas Propag.*, vol. 58, no. 3, pp. 963–966, Mar. 2010.

[14] J. Cheng and A. Alphones, “Leaky-wave radiation behavior from a double periodic composite right/left-handed substrate integrated waveguide,” *IEEE Trans. Antennas Propag.*, vol. 60, no. 4, pp. 1727–1735, Apr. 2012.

[15] J. Liu, X. Tang, Y. Li, and Y. Long, “Substrate integrated waveguide leaky-wave antenna with H-shaped slots,” *IEEE Trans. Antennas Propag.*, vol. 60, no. 8, pp. 3962–3967, Aug. 2012.

[16] J. Liu and Y. Long, “Analysis of a microstrip leaky-wave antenna loaded with shorted stubs,” *IEEE Antennas Wireless Propag. Lett.*, vol. 7, pp. 501–504, Dec. 2008.

[17] Y. Li, Q. Xue, H.-Z. Tan, and Y. Long, “The half-width microstrip leaky wave antenna with the periodic short circuits,” *IEEE Trans. Antennas Propag.*, vol. 59, no. 9, pp. 3421–3423, Sep. 2011.

[18] Y. Ning, C. Caloz, and K. Wu, “Full-space scanning periodic phase-reversal leaky-wave antenna,” *IEEE Trans. Microw. Theory Techn.*, vol. 58, no. 10, pp. 2619–2632, Oct. 2010.

[19] G.-F. Cheng and C.-K. C. Tzuang, “A differentially excited coupled half-width microstrip leaky EH_1 mode antenna,” *IEEE Trans. Antennas Propag.*, vol. 61, no. 12, pp. 5885–5892, Dec. 2013.

[20] M. Archbold, E. J. Rothwell, L. C. Kempel, and S. W. Schneider, “Beam steering of a half-width microstrip leaky-wave antenna using edge loading,” *IEEE Antennas Wireless Propag. Lett.*, vol. 9, pp. 203–206, Apr. 2010.

[21] A. Suntives and S. V. Hum, “A fixed-frequency beam-steerable half-mode substrate integrated waveguide leaky-wave antenna,” *IEEE Trans. Antennas Propag.*, vol. 60, no. 5, pp. 2540–2544, May 2012.

[22] A. Pourghorban Saghati, M. M. Mirsalehi, and M. H. Neshati, “A HMSIW circularly polarized leaky-wave antenna with backward, broadside, and forward radiation,” *IEEE Antennas Wireless Propag. Lett.*, vol. 13, pp. 451–454, Mar. 2014.

[23] Nasimuddin, Z. N. Chen, and X. Qing, “Substrate integrated metamaterial-based leaky-wave antenna with improved boresight radiation bandwidth,” *IEEE Trans. Antennas Propag.*, vol. 61, no. 7, pp. 3451–3457, Jul. 2013.

[24] Y. Mohtashami and J. Rashed-Mohassel, “A butterfly substrate integrated waveguide leaky-wave antenna,” *IEEE Trans. Antennas Propag.*, vol. 62, no. 6, pp. 3384–3388, Jun. 2014.

[25] J. Liu, D. R. Jackson, Y. Li, C. Zhang, and Y. Long, “Investigations of SIW leaky-wave antenna for endfire-radiation with narrow beam and sidelobe suppression,” *IEEE Trans. Antennas Propag.*, vol. 62, no. 9, pp. 4489–4497, Sep. 2014.

[26] J. Liu, D. R. Jackson, and Y. Long, “Substrate integrated waveguide (SIW) leaky-wave antenna with transverse slots,” *IEEE Trans. Antennas Propag.*, vol. 60, no. 1, pp. 20–29, Jan. 2012.

[27] R. Guzman-Quiros, J. L. Gomez-Tornero, A. R. Weily, and Y. J. Guo, “Electronically steerable 1-D Fabry-Perot leaky-wave antenna employing a tunable high impedance surface,” *IEEE Trans. Antennas Propag.*, vol. 60, no. 11, pp. 5046–5055, Nov. 2012.

[28] J. L. Gomez-Tornero, “Analysis and design of conformal tapered leaky-wave antennas,” *IEEE Antennas Wireless Propag. Lett.*, vol. 10, pp. 1068–1071, Oct. 2011.

[29] C. Luxey and J.-M. Latheurte, “Simple design of dual-beam leaky-wave antennas in microstrips,” *IEE Proc. Microw. Antennas Propag.*, vol. 144, no. 6, pp. 397–402, Dec. 1997.

[30] R. O. Ouedraogo, E. J. Rothwell, and B. J. Greetis, “A reconfigurable microstrip leaky-wave antenna with a broadly steerable beam,” *IEEE Trans. Antennas Propag.*, vol. 59, no. 8, pp. 3080–3083, Aug. 2011.

[31] Y. Li, Q. Xue, E. K.-N. Yung, and Y. Long, “Dual-beam steering microstrip leaky wave antenna with fixed operating frequency,” *IEEE Trans. Antennas Propag.*, vol. 56, no. 1, pp. 248–252, Jan. 2008.

[32] Y.-D. Lin, P.-M. Chi, and T.-L. Chen, “Design of the feeding structures for the excitation of the microstrip line second higher order mode leaky-wave antenna,” in *Proc. IEEE Antennas Propag. Soc. Int. Symp. Dig.*, Jul. 1997, pp. 1142–1145.

[33] T.-L. Chen and Y.-D. Lin, “Aperture-coupled microstrip second higher order leaky-mode antenna,” in *Proc. Asia-Pac. Microw. Conf. (APMC)*, 2001, pp. 1060–1063.

[34] J. L. Gomez-Tornero, D. Caete-Rebenaque, and A. Alvarez-Melcon, “Microstrip leaky-wave antenna with control of leakage rate and only one main beam in the azimuthal plane,” *IEEE Trans. Antennas Propag.*, vol. 56, no. 2, pp. 335–344, Feb. 2008.

[35] C.-C. Lin and C.-K. C. Tzuang, “A dual-beam micro-CPW leaky-mode antenna,” *IEEE Trans. Antennas Propag.*, vol. 48, no. 2, pp. 310–316, Feb. 2000.

[36] G. M. Zelinski, G. A. Thiele, M. L. Hastriter, M. J. Havrilla, and A. J. Terzuoli, “Half width leaky wave antennas,” *IET Microw. Antennas Propag.*, vol. 1, no. 2, pp. 341–348, Apr. 2007.

[37] C. Caloz, D. R. Jackson, and T. Itoh, “Leaky-wave antennas,” in *Frontiers in Antennas*, F. B. Gross, Ed. New York, NY, USA: McGraw-Hill, 2011, ch. 9.

[38] A. A. Oliner and D. R. Jackson, “Leaky-wave antennas,” in *Antenna Engineering Handbook*, J. L. Volakis, Ed. New York, NY, USA: McGraw-Hill, 2007, ch. 11.

Debabrata K. Karmokar (S’12–M’15) was born in Satkhira, Bangladesh. He received the B.Sc. degree in electrical and electronic engineering (EEE) from the Khulna University of Engineering and Technology (KUET), Khulna, Bangladesh, in 2007, and the Ph.D. degree in electronic engineering from Macquarie University, Sydney, NSW, Australia, in 2015.

In 2007, he joined the Department of Electrical and Electronic Engineering, KUET, as a Lecturer and became an Assistant Professor in 2011. He was an Assistant Director of Students’ Welfare of KUET where he was responsible for different administrative activities of the university, and a Member of Consultancy, Research and Testing Services (CRTS) of the Department of EEE, KUET. He was a Secretary of the IEEE Student Branch, Macquarie University. He has authored/coauthored over 55 journal and conference papers. His research interests include leaky-wave antennas (LWAs), metamaterial-based antennas, reconfigurable antennas, ultra-wideband (UWB) antennas, broadband and multiband printed antennas, electromagnetic band gap (EBG) resonator antennas, dielectric-resonator antennas, and wireless power transfer.

Dr. Karmokar serving as a Reviewer for several journals including the IEEE Antennas and Wireless Propagation Letters and the *IET Microwaves, Antennas, and Propagation*. His biography has been included in Marquis *Who’s Who in the World* 2016 (33rd Edition). He was the recipient of the Commonwealth-funded International Postgraduate Research Scholarship (IPRS), the International Macquarie University Research Excellence Scholarship (iMQRES) from Macquarie University, and the OCE Ph.D. Scholarship from the Commonwealth Scientific and Industrial Research Organisation (CSIRO) ICT Centre, Marsfield, Australia. He won the First Prize in Poster Competition in Engineering Symposium 2015, Macquarie University, Australia.

Karu P. Esselle (M'92–SM'96–F'16) received the B.Sc. (with First Class Hons.) degree in electronic and telecommunication engineering from the University of Moratuwa, Moratuwa, Sri Lanka, and the M.A.Sc. and Ph.D. degrees in electrical engineering from the University of Ottawa, Ottawa, ON, Canada.

He is a Professor of electronic engineering with Macquarie University, Sydney, Australia, and the Past Associate Dean—Higher Degree Research (HDR) of the Division of Information and Communication Sciences. He has authored about 450 research publications and his papers have been cited more than 3200 times. His current Google Scholar h-index of 29 is the all-time highest among Australian antenna researchers, when Google Scholar errors are corrected. Since 2002, his research team has been involved with research grants, contracts, and Ph.D. scholarships worth over 15 million dollars. His research has been funded by many national and international organizations including Australian Research Council, Intel, US Air Force, Cisco Systems and Hewlett-Packard, and Australian and Indian governments.

Prof. Esselle is an Associate Editor of IEEE Access and IET Microwave, Antennas, and Propagation. He is the Technical Program Committee Co-Chair of ISAP 2015, APMC 2011, and TENCON 2013 and the Publicity Chair of ICEAA 2016, IWAT 2014, and APMC 2000. He is the Foundation Counsellor of IEEE Student Branch at Macquarie University, and Foundation Advisor of IEEE MTT Chapter in Macquarie University. He has also served as a Member of the Dean's Advisory Council and the Division Executive from 2003 to 2008 and as the Head of the Department several times. He is the Chair of the Board of Management, Australian Antenna Measurement Facility, Deputy Director (Engineering) of the WiMed Research Centre, and elected 2016 Chair of both IEEE New South Wales (NSW) Section, and IEEE NSW AP/MTT Chapter. He directs the Centre for Collaboration in Electromagnetic and Antenna Engineering. When he was elected to the IEEE Antennas and Propagation Society Administrative Committee for a three year term in 2014, he became the only person residing in the Asia-Pacific Region (IEEE Region 10) to be elected to this highly competitive position over a period of at least six years (2010–2015). He was elevated to IEEE Fellow grade for his extensive contributions to resonance-based antennas, both low gain, and high gain. He has been invited to serve as an International Expert/Research Grant Assessor by several nationwide research funding bodies overseas including the Netherlands, Canada, Finland, Hong-Kong, Georgia, and Chile. He has been invited by Vice-Chancellors of Australian and overseas universities to assess applications for promotion to professorial levels. He has provided expert assistance to more than a dozen companies including Intel, Hewlett Packard Laboratory (USA), Cisco Systems (USA), Cochlear, Optus, ResMed, and Katherine-Werke (Germany). He has also been invited to assess grant applications submitted to Australia's most prestigious schemes such as Australian Federation Fellowships and Australian Laureate Fellowships. He leads the Implantable Wireless Program of the WiMed Research Centre. In addition to the large number of invited conference speeches he has given, he has been an invited keynote speaker of IEEE workshops and conferences. His mentees have been awarded with many fellowships, awards, and prizes for their research achievements. Thirty-one international experts who examined the theses of his recent Ph.D. graduates ranked them in the top 5% or 10%. He was the recipient of the 2012 Best Published Paper Award in Electronic and Telecommunication Engineering from IESL NSW Chapter, the 2011 Outstanding Branch Counsellor Award from IEEE headquarters (USA), the 2009 Vice Chancellor's Award for Excellence in Higher Degree Research Supervision, and the 2004 Inaugural Innovation Award for best invention disclosure. Professor Esselle's research activities are posted in the web at http://web.science.mq.edu.au/~esselle/.

Trevor S. Bird (S'71–M'76–SM'85–F'97–LF'15) received the B.App.Sc., M.App.Sc., and Ph.D. degrees from the University of Melbourne, Parkville, Vic., Australia, in 1971, 1973, and 1977, respectively.

He was a Postdoctoral Research Fellow with Queen Mary College, University of London, London, U.K., for two years, followed by five years as a Lecturer in the Department of Electrical Engineering, James Cook University, Douglas, Australia. From 1982 to 1983, he was a Consultant with Plessey Radar, London, U.K., before joining the Commonwealth Scientific and Industrial Research Organisation (CSIRO), Sydney, Australia, in 1983. He held several positions with CSIRO, including Chief Scientist, ICT Centre. He is currently Principal of Antengenuity, a specialist consulting firm, an Honorary CSIRO Fellow; and an Adjunct Professor with Macquarie University, North Ryde, Australia.

Dr. Bird is a Fellow of the Australian Academy of Technological and Engineering Sciences, the Institution of Electrical Technology (IET), Queens College, University of Melbourne, and an Honorary Fellow of the Institution of Engineers, Australia. He was a Distinguished Lecturer for the IEEE Antennas and Propagation Society from 1997 to 1999; a Chair of the New South Wales joint AP/MTT Chapter from 1995 to 1998, and again in 2003; the Chairman of the 2000 Asia Pacific Microwave Conference; a Member of the New South Wales Section Committee from 1995–2005 and was Vice-Chair and Chair of the Section in 1999–2000 and 2001–2002, respectively; an Associate Editor of the IEEE TRANSACTIONS ON ANTENNAS AND PROPAGATION from 2001 to 2004; a Member of the Administrative Committee of the IEEE Antennas and Propagation Society from 2003 to 2005; the Editor-in-Chief of the IEEE TRANSACTIONS ON ANTENNAS AND PROPAGATION from 2004 to 2010; and the President of the Society on 2013. He was a member of the College of Experts of the Australian Research Council (ARC) in 2006–2007 and also a Member of the technical committee of numerous conferences including JINA, ICAP, AP2000, IRMMW-THz, and the URSI Electromagnetic Theory Symposium. Currently, he is member of the Editorial Boards of the IET Microwaves Antennas and Propagation. Since 2006, his biography has been listed in Who's Who in Australia. He was the recipient of the John Madsen Medal of the Institution of Engineers, Australia, on four occasions for the Best Paper published annually in the *Journal of Electrical and Electronic Engineering*; the corecipient of the H.A. Wheeler Applications Prize Paper Award of the IEEE Antennas and Propagation Society, in 2001; the CSIRO Medals for achievement in 1990, 1998, and 2011; an IEEE Third Millennium Medal for outstanding contributions to the IEEE New South Wales Section, in 2000; project awards from the Society of Satellite Professionals International (New York) in 2004; the Engineers Australia in 2001; the Communications Research Laboratory, Japan, in 2000; a Centenary Medal for service to Australian society in telecommunications and was also named Professional Engineer of the Year by the Sydney Division, Engineers Australia, in 2003; the M.A. Sargent Medal in 2012 by Engineers Australia for sustained contributions to electrical engineering.